
Properties of Stars

*When quacks with pills political would dope us,
When politics absorbs the livelong day,
I like to think about that star Canopus,
So far, so far away.*

*Greatest of visioned suns, they say who list 'em;
To weigh it science almost must despair.
Its shell would hold our whole dinged solar system,
Nor even know 'twas there.*

Bert Leston Taylor (1866–1921)
“Canopus” [1913]

A star can be defined as a self-gravitating ball of gas, usually spherical or spheroidal, that is powered by nuclear fusion in its interior. In this text, we will go slightly beyond the boundaries of this definition to discuss protostars and pre-main sequence stars (not yet powered by fusion), stellar remnants (no longer powered by fusion), and brown dwarfs (too small to be powered by fusion).

Less than 10% of the baryonic matter in the universe is contained in stars; less than 5% of the mass-energy of the universe is in the form of baryonic matter. Thus, stars make up less than 0.5% of the universe. Why do we devote an entire astrophysics textbook to such a small fraction of the universe? In part, we are simply following the well-trodden path of our astronomical ancestors. It wasn't until the twentieth century that astronomers were able to make extensive observations outside the visible range of the spectrum ($\lambda = 4000 \text{ \AA} - 7500 \text{ \AA}$). Since human eyes evolved to take advantage of light emitted by a star, it isn't surprising that our eyes are quite good at detecting stars. Before the development of detectors that worked outside the visible range, astronomers had to study stars, and objects that reflect starlight, because that was what they could see.

However, even when we open our eyes (metaphorically) to the full spectrum of electromagnetic radiation, stars are well worth studying. The average mass density of baryonic matter today is $\rho_{\text{bary},0} = 4.2 \times 10^{-31} \text{ g cm}^{-3}$. The average density

of the Sun is $\rho_{\odot} = 1.410 \text{ g cm}^{-3}$, over 30 orders of magnitude greater than the baryonic density of the universe as a whole. When gas is compressed to such high densities, interesting physical processes, such as nuclear fusion, can occur. How does a self-gravitating fusion reactor regulate itself? How does the released energy escape from the self-gravitating fusion reactor? What happens when the self-gravitating fusion reactor runs out of fuel? How is the self-gravitating fusion reactor assembled from the low-density gas of interstellar space? How does rotation affect the self-gravitating fusion reactor's structure?

All these questions will be dealt with in this text; however, let's replace the phrase "self-gravitating fusion reactor" with the word "star," for the sake of brevity.

1.1 Observing the Sun

For those of us living on or near the Earth, the most easily observed star is the Sun. Many generations of astronomers have attempted to determine the length of the astronomical unit (au), originally defined as the average distance from the Earth's center to the Sun's center. Geometric methods, such as diurnal parallax, gave way to radar and to radio telemetry of interplanetary spacecraft. By the twenty-first century, the debate over how to correct for relativistic effects and for the gradually increasing size of the Earth's orbit (resulting from the Sun's mass-energy loss) became frustratingly tangled. Cutting the Gordian knot, the International Astronomical Union (IAU) resolved that the astronomical unit be defined as a conventional unit of length, with $1 \text{ au} \equiv 149\,597\,870.7 \text{ km}$. For our purposes, we can state that the length of the semimajor axis of the Earth's orbit is $a = 1 \text{ au}$, and that the perihelion and aphelion distances are $r_{\text{pe}} = 0.9833 \text{ au}$ and $r_{\text{ap}} = 1.0167 \text{ au}$.

The angular diameter of the Sun as seen from Earth ranges from $\theta_{\text{pe}} = 1951 \text{ arcsec}$ at perihelion to $\theta_{\text{ap}} = 1887 \text{ arcsec}$ at aphelion. The radius of the Sun in physical units is thus

$$R_{\odot} = r_{\text{ap}} \tan\left(\frac{\theta_{\text{ap}}}{2}\right) = r_{\text{pe}} \tan\left(\frac{\theta_{\text{pe}}}{2}\right) \approx 0.00465 \text{ au} \approx 696\,000 \text{ km}. \quad (1.1)$$

This calculation assumes that the Sun has a well-defined radius, despite being a ball of gas rather than a ball of solid rock. In fact, a broadband optical image of the Sun, as seen in Figure 1.1, does have rather well-defined edges. This is because most of the visible light from the Sun comes from the thin **photosphere**, a layer that is only $\sim 400 \text{ km}$ thick. Quoting a single radius R_{\odot} for the Sun also implicitly assumes that the Sun is spherical. Fortunately, this approximation is an excellent one. Although the Sun does have a measurable oblateness, its polar radius is smaller than its equatorial radius by only 5 km , representing a difference of less than one part in 10^5 . Given that the Sun is continuously quivering (as a

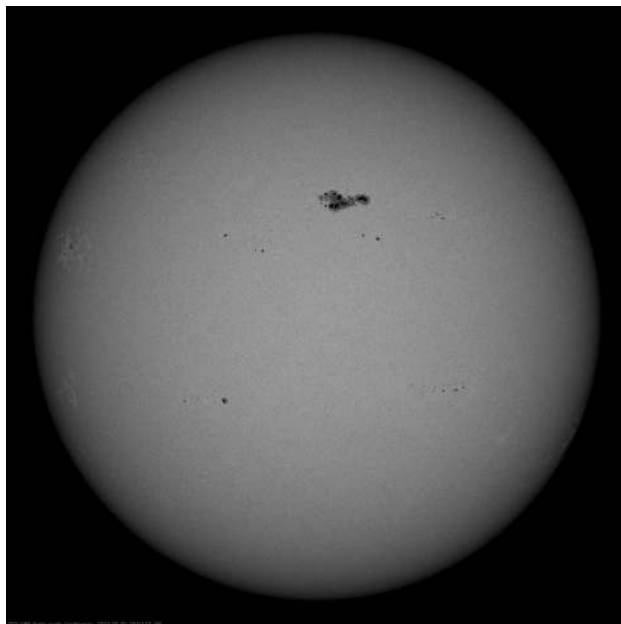


Figure 1.1 An image of the Sun at visible wavelengths, taken on 2022 May 20, when the Sun had a sunspot group in one hemisphere. [Courtesy of NASA/SDO and HMI science team]

result of seismic waves), and that it is slowly expanding as it evolves, the IAU has recommended the use of a “nominal solar radius,” defined as

$$1 R_{\odot}^N \equiv 695\,700 \text{ km.} \quad (1.2)$$

This is the value for the solar radius that we will use in this text.¹

The solar image in Figure 1.1 shows a number of dark **sunspots** in the Sun’s photosphere. Sunspots are regions where the Sun’s magnetic field is much stronger than average. A typical magnetic field strength in the Sun’s photosphere is $B_{\odot} \sim 3 \text{ G}$; in a sunspot, however, the field strength can be as high as $B_{\text{spot}} \sim 3000 \text{ G}$. Sunspots appear dark because they are cooler than the surrounding photosphere. While the average photospheric temperature is $T \sim 5800 \text{ K}$, the temperature at the center of a sunspot can be as low as $T \sim 3900 \text{ K}$. (The resulting lower gas pressure within the sunspot compensates for its higher magnetic pressure, and the sunspot remains in pressure equilibrium with the surrounding photosphere.)

The existence of sunspots, which drift only gradually in solar latitude and longitude, permits us to measure the Sun’s rotation period. Galileo, for instance, used his sunspot observations to estimate that the Sun’s rotation period was roughly

¹ The use of a nominal solar radius enables us to make statements such as “When the Sun becomes a red giant, the Sun’s radius will be 2.4 solar radii” without causing rampant confusion.

equal to one month (“mese lunare”), or 29 days. Subsequent observations revealed that the Sun is in differential rotation, with a period that ranges from $\mathcal{P}_{\text{rot}} = 24.5$ d at its equator to $\mathcal{P}_{\text{rot}} = 27.5$ d at latitude $\ell = \pm 45^\circ$. (It’s hard to use sunspots to determine the rotation period at higher latitudes, since spots stay fairly close to the equator.) The equatorial rotation period $\mathcal{P}_\odot = 24.5$ d corresponds to an angular speed of $\Omega_\odot = 2\pi/\mathcal{P}_\odot = 2.97 \times 10^{-6} \text{ s}^{-1}$ and a rotation speed of $v_\odot = \Omega_\odot R_\odot = 2.07 \text{ km s}^{-1}$.

From the size of the Earth’s orbit, $a = 1 \text{ au} = 1.49598 \times 10^{13} \text{ cm}$, and the length of the sidereal year, $\mathcal{P} = 365.256 \text{ d} = 3.15581 \times 10^7 \text{ s}$, we can use Kepler’s third law, as modified by Newton, to find

$$GM_\odot = \frac{4\pi^2 a^3}{\mathcal{P}^2} = 1.3271 \times 10^{26} \text{ cm}^3 \text{ s}^{-2}, \quad (1.3)$$

where M_\odot is the mass of the Sun and G is Newton’s gravitational constant. (The mass of the Earth, which is three parts per million of the Sun’s mass, can be ignored at this level of accuracy.) The product GM_\odot , known as the solar mass parameter, is better known than G and M_\odot are individually. In fact, the IAU has recommended a “nominal solar mass parameter,” defined as

$$1 (GM_\odot)^N \equiv 1.3271244 \times 10^{26} \text{ cm}^3 \text{ s}^{-2}. \quad (1.4)$$

Using the best available value for the gravitational constant,² $G = 6.6743 \times 10^{-8} \text{ cm}^3 \text{ g}^{-1} \text{ s}^{-2}$, we find that the nominal solar mass parameter implies

$$1 M_\odot = 1.9884 \times 10^{33} \text{ g}. \quad (1.5)$$

This is the value for the solar mass that we will use in this text.

The mass of the Sun is currently decreasing because of the **solar wind**, an outflow of charged particles from the Sun’s extended hot corona. Satellites sent beyond the Earth’s magnetosphere have studied the density, speed, and composition of the solar wind. The particles of the solar wind are mainly electrons and protons, with a smaller number of ^4He nuclei and other heavier ions. The solar wind is “gusty,” with fluctuations in its density and speed. However, averaged over time, the Sun’s mass loss rate from the solar wind is $\dot{M}_{\text{wind}} \approx 1.2 \times 10^{12} \text{ g s}^{-1} \approx 2.0 \times 10^{-8} M_\odot \text{ Myr}^{-1}$.

At any given instant, the **solar irradiance** is the energy flux of sunlight, integrated over all frequencies, incident on a plane perpendicular to the Sun’s rays at a distance of 1 au from the Sun. Since the Earth’s atmosphere is very good at absorbing some frequencies of light, the solar irradiance can be measured accurately only by satellites. As shown in Figure 1.2, the solar irradiance varies with time over the solar activity cycle of ~ 11 yr. At solar minimum, when the Sun has few sunspots, flares, or plages (bright regions near sunspots), the solar irradiance is $1.3606 \times 10^6 \text{ erg s}^{-1} \text{ cm}^{-2}$, with little variation from day to day; at

² This is the 2018 CODATA recommended value for G , with a relative standard uncertainty of 22 parts per million.

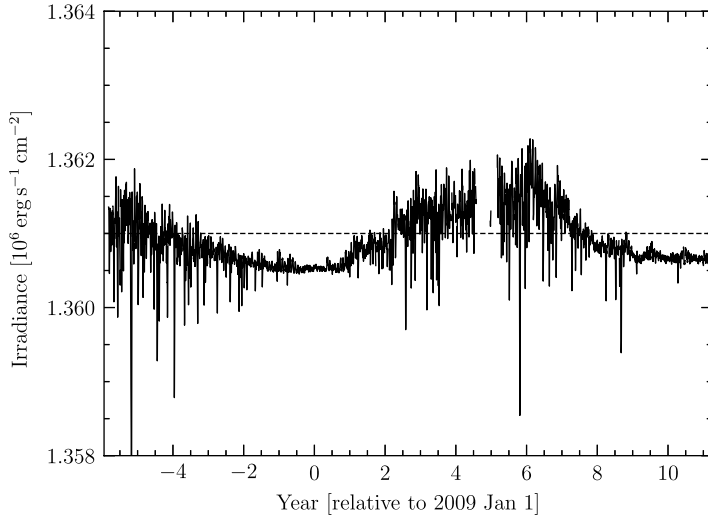


Figure 1.2 Solar irradiance from 2003 Feb to 2020 Feb, when the *Solar Radiation and Climate Experiment (SORCE)* satellite was in operation. During this time, solar minima occurred around 2008 Dec and 2019 Dec, while a solar maximum occurred around 2014 Apr. [Data from *SORCE*]

solar maximum, it averages $1.3614 \times 10^6 \text{ erg s}^{-1} \text{ cm}^{-2}$, with a larger variation. It may seem counterintuitive that the Sun produces more light when it is covered with cool sunspots at solar maximum; however, the increased light from flares and plagues at solar maximum more than makes up for the decreased light from sunspots.

The solar irradiance averaged over a complete solar cycle is called the **solar constant**. A value of $S_{\odot} = 1.361 \times 10^6 \text{ erg s}^{-1} \text{ cm}^{-2}$ is typically adopted for the solar constant. This value yields a computed **solar luminosity** of

$$1 L_{\odot} = 4\pi a^2 S_{\odot} = 3.828 \times 10^{33} \text{ erg s}^{-1}. \quad (1.6)$$

This is equal to the IAU’s recommended “nominal solar luminosity,” and is the value for the solar luminosity that we will use in this text. In addition to emitting photons from its superficial photosphere, the Sun also emits neutrinos from its core. The Sun’s *neutrino* luminosity is $L_{\nu,\odot} \approx 0.023 L_{\odot}$. The equivalent mass loss rate of all the photons and neutrinos that the Sun tosses away into space is

$$\dot{M}_{\text{rad}} = \frac{L_{\odot} + L_{\nu,\odot}}{c^2} = 4.36 \times 10^{12} \text{ g s}^{-1} = 6.92 \times 10^{-8} M_{\odot} \text{ Myr}^{-1}. \quad (1.7)$$

Thus, the loss of radiation provides more than three-quarters of the Sun’s mass-energy loss, with the solar wind making only a minority contribution. The total mass loss rate of the Sun is

$$\dot{M}_{\odot} = \dot{M}_{\text{wind}} + \dot{M}_{\text{rad}} \approx 8.9 \times 10^{-8} M_{\odot} \text{ Myr}^{-1}, \quad (1.8)$$

leading to a characteristic mass loss time $M_{\odot}/\dot{M}_{\odot} \approx 11\,000 \text{ Gyr}$.

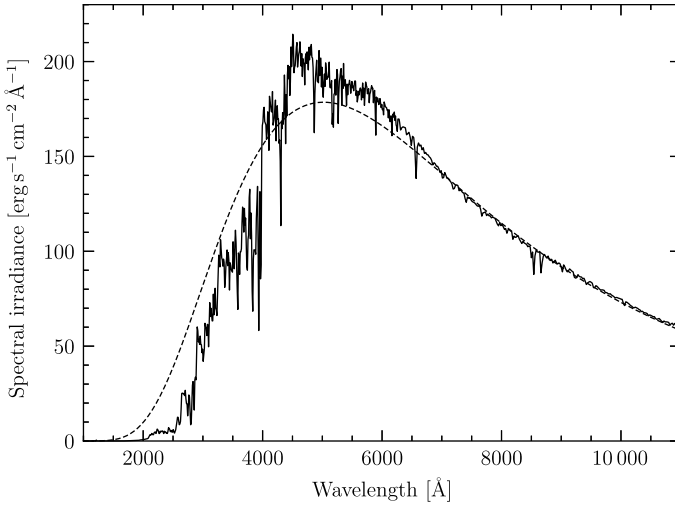


Figure 1.3 The solar spectrum as seen 1 au from the Sun, without filtering by the Earth’s atmosphere. The dashed line shows a blackbody spectrum with a temperature $T = 5772$ K. [ASTM E-490-00 solar spectrum]

An effective temperature $T_{\text{eff},\odot}$ for the Sun’s photosphere can be computed from the relation

$$L_{\odot} = 4\pi R_{\odot}^2 \sigma_{\text{SB}} T_{\text{eff},\odot}^4, \quad (1.9)$$

where $\sigma_{\text{SB}} = 5.6704 \times 10^{-5} \text{ erg cm}^{-2} \text{ s}^{-1} \text{ K}^{-4}$ is the Stefan–Boltzmann constant. (In other words, the Sun’s effective temperature is the temperature of a perfect blackbody with the same luminosity and surface area as the Sun.) Using the IAU nominal values for the solar radius and solar luminosity, the effective temperature of the Sun is

$$T_{\text{eff},\odot} = \left(\frac{L_{\odot}}{4\pi R_{\odot}^2 \sigma_{\text{SB}}} \right)^{1/4} = 5772 \text{ K}. \quad (1.10)$$

Although for some purposes the Sun may be safely approximated as a blackbody with $T = T_{\text{eff},\odot} = 5772$ K, the detailed spectrum of the Sun, shown in Figure 1.3, is not extremely close to that of a blackbody. In particular, the Sun’s spectrum is ultraviolet-deficient compared to a blackbody with $T = 5772$ K. The blackbody approximation is better in the near infrared, where there are fewer absorption lines in the Sun’s spectrum.

The absorption lines in the solar spectrum give us information on the elements present in the photosphere. For instance, the existence of hydrogen is revealed by the presence of the hydrogen Balmer lines: $H\alpha$ at $\lambda = 6563 \text{ \AA}$, $H\beta$ at $\lambda = 4861 \text{ \AA}$, and so forth. However, determining the relative abundance of elements in the Sun is not a straightforward process. Some elements do not have detectable photospheric absorption lines; for instance, helium was first discovered from its emission lines in the Sun’s chromosphere, the hotter layer just above the

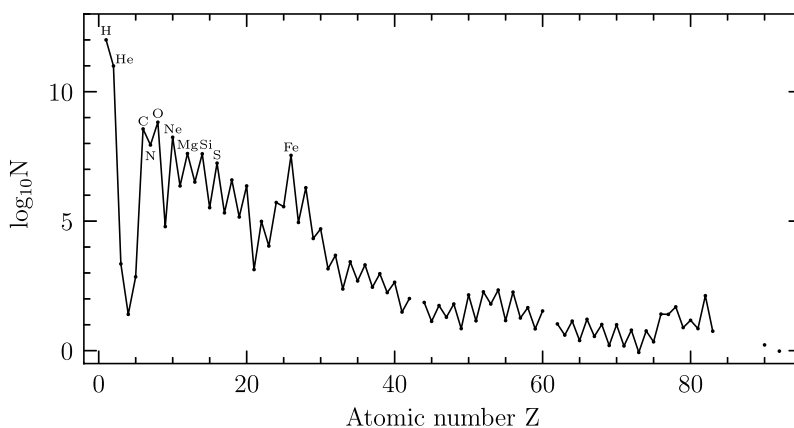


Figure 1.4 Abundances (by number) of elements present in the Sun at its formation; abundances are normalized to $N(\text{H}) = 10^{12}$ hydrogen atoms. The 10 most abundant elements are labeled. [Data from Lodders 2021]

photosphere. In addition, the abundances in the Sun's photosphere today are not the same as the abundances the Sun started with. Heavy elements settle slowly inward through diffusion, while unstable elements such as uranium undergo decay. Taking into account these effects, Figure 1.4 shows the reconstructed abundances of the protosolar nebula from which the Sun formed 4.57 Gyr ago.

Figure 1.4 doesn't display all the information that we have about protosolar abundances. In particular, it bins together all the different isotopes of each element. It is admittedly true that the most common elements are overwhelmingly made of a single isotope. For instance, in the protosolar nebula, hydrogen was 99.998% ordinary hydrogen (^1H) and only 0.002% deuterium (^2H) by number, while helium was 99.983% ordinary helium (^4He) and only 0.017% light helium (^3He). However, as we discuss in Section 5.3, the amount of ^2H and ^3He present in a star provides a useful probe of nuclear fusion conditions. Thus, we do sometimes care about scarce isotopes. (In addition, some elements do not have an overwhelmingly dominant isotope; for instance, bromine is 50.7% ^{79}Br and 49.3% ^{81}Br by number.)

By contrast, other astrophysical problems are largely indifferent to the exact details of elemental and isotopic abundances. For these problems, we need only three broad categories: (1) hydrogen, (2) helium, and (3) all other elements combined. Suppose that the mass density of gas is ρ , the number density of hydrogen nuclei is n_{H} , and the number density of helium nuclei is n_{He} . The mass of a hydrogen atom is $m_{\text{H}} = 1.674 \times 10^{-24}$ g; at solar abundance, the presence of ^2H raises the mean atomic mass by only 1 part in 25 000. The mass of a helium atom is $m_{\text{He}} = 6.646 \times 10^{-24}$ g; at solar abundance, the presence of ^3He lowers the mean atomic mass by only 1 part in 8000. Knowing the atomic masses, we can convert from the number density n_{H} to the mass fraction of hydrogen,

$$X \equiv \frac{n_{\text{H}}m_{\text{H}}}{\rho}, \quad (1.11)$$

and from the number density n_{He} to the mass fraction of helium,

$$Y \equiv \frac{n_{\text{He}}m_{\text{He}}}{\rho}. \quad (1.12)$$

This means that the mass fraction of “metals,” or all heavier elements combined,³ is

$$Z \equiv 1 - X - Y. \quad (1.13)$$

The protosolar abundances are estimated to have been $X_{\odot,0} = 0.706$, $Y_{\odot,0} = 0.277$, and $Z_{\odot,0} = 0.017$. In the Sun’s photosphere today, after diffusive settling of elements heavier than hydrogen, the abundances are $X_{\odot} = 0.739$, $Y_{\odot} = 0.246$, and $Z_{\odot} = 0.015$. The most abundant metal in the Sun is oxygen, which contributed about 43% of the protosolar metal mass. Carbon provided 18%, neon provided 14%, and iron provided 8% of the metallicity by mass. (For comparison with the solar values, the primordial abundances that came out of Big Bang Nucleosynthesis were $X_{\text{p}} \approx 0.753$ and $Y_{\text{p}} \approx 0.247$; the primordial mass fraction of metals was $Z_{\text{p}} \approx 3 \times 10^{-9}$, mostly in the form of ${}^7\text{Li}$.)

Because we know the Sun better than we know any other star, our standard unit of length will be the solar radius, with $1 R_{\odot} = 6.957 \times 10^{10}$ cm, our standard unit of mass will be the solar mass, with $1 M_{\odot} = 1.9884 \times 10^{33}$ g, and our standard unit of power will be the solar luminosity, with $1 L_{\odot} = 3.828 \times 10^{33}$ erg s⁻¹. (Since the Sun’s volume is $V_{\odot} = 4\pi R_{\odot}^3/3 = 1.410 \times 10^{33}$ cm³, we have the useful mnemonic that the Sun’s most important properties are all $\sim 10^{33}$ in cgs units.)

1.2 Observing Other Stars

Determining the properties of stars other than the Sun is frequently made difficult by their large distance. The most reliable method of finding the distance to the nearest stars is trigonometric parallax. As seen from Earth over the course of one year, the apparent motion of a star on the sky can be fitted as a combination of linear proper motion (from the star’s motion relative to the Sun) and a parallactic ellipse (from the Earth’s orbital motion around the Sun). The semimajor axis of the ellipse, in angular units, is the parallax p of the star. The parallax is related to the star’s distance in parsecs (pc) by the equation

$$\frac{d}{1 \text{ pc}} = \frac{1 \text{ arcsec}}{p}. \quad (1.14)$$

³ Astronomers commonly use the term “metals” to mean “elements other than hydrogen or helium.” A metallurgist might well be annoyed by this misuse of the word “metal,” but we will accept it as a colorful metaphor and move onward.

Given this relation, $1 \text{ pc} = 206\,265 \text{ au}$, just as $1 \text{ radian} = 206\,265 \text{ arcsec}$. As an example, the nearby star Proxima Centauri has a parallax $p_{\text{prox}} = 0.768\,07 \text{ arcsec}$. This parallax implies a distance $d_{\text{prox}} = 1/p_{\text{prox}} = 1.3020 \text{ pc}$; this can also be expressed as $d_{\text{prox}} = 268\,550 \text{ au}$.⁴

Proxima Centauri is famously the Sun's nearest neighbor among the stars. Measuring accurate parallaxes for significantly more distant stars typically requires dedicated space-based missions. For instance, the *Gaia* spacecraft was launched in 2013 with the goal of measuring the parallax of $\sim 10^9$ stars, with an accuracy ranging from $\sigma_p \sim 10^{-5} \text{ arcsec} \sim 0.01 \text{ mas}$ for the apparently brightest stars in its sample to $\sigma_p \sim 0.3 \text{ mas}$ for the faintest.

Measuring the angular diameter of stars, given their large distances, typically requires interferometric techniques. The star (other than the Sun) that has the largest angular size as seen from Earth is R Doradus, a red variable star. Its angular diameter has been measured in the near infrared using aperture masking interferometry, with the result $\theta_{\text{RD}} = 57 \pm 5 \text{ mas}$. Its parallax is $p_{\text{RD}} = 18.31 \pm 0.99 \text{ mas}$, yielding a distance $d_{\text{RD}} = 54.6 \pm 3.0 \text{ pc}$. Together, these values imply a physical radius $R_{\text{RD}} = 1.56 \pm 0.16 \text{ au}$. Thus, R Doradus is physically much larger than the Sun, with $R_{\text{RD}} \approx 330 R_{\odot}$.

R Doradus is far from being the largest star in our galaxy. Consider Betelgeuse (α Orionis), which is also a red variable star. The diameter of Betelgeuse varies with time; in the year 2019, measurements in the near infrared gave an angular diameter of $\theta_{\text{bet}} = 42.61 \pm 0.05 \text{ mas}$.⁵ The parallax of Betelgeuse is poorly known, in part because p_{bet} is small compared to the angular size θ_{bet} , and in part because Betelgeuse is variable in shape as well as size. If we assume $p_{\text{bet}} = 5.5 \pm 1.0 \text{ mas}$, consistent with recent measurements, this implies a physical radius of $R_{\text{bet}} = 3.9 \pm 0.7 \text{ au}$. Thus, the radius of Betelgeuse is $R_{\text{bet}} \sim 2.5 R_{\text{RD}} \sim 800 R_{\odot}$. Resolved images of Betelgeuse have been taken at visible and ultraviolet wavelengths, as seen in Figure 1.5; however, these images include the extended outer atmosphere of Betelgeuse (which is perceptibly non-spherical). The ultraviolet angular diameter of Betelgeuse, as shown in the right panel of Figure 1.5, is $\theta_{\text{uv}} \approx 120 \text{ mas}$, nearly three times the size of the near-infrared photosphere of Betelgeuse; this corresponds to a physical radius of $R_{\text{uv}} \sim 11 \text{ au}$ for the UV-emitting outer atmosphere.

Although the Sun is small compared to R Doradus and Betelgeuse, it is by no means a midget among stars. Consider, for instance, the stars of the α Centauri system. Within this triple star system, Proxima Centauri (at $d = 1.302 \text{ pc}$ from the Sun) is loosely bound to the tight binary α Centauri AB (at $d = 1.332 \text{ pc}$). Using interferometric techniques, the angular diameter of α Centauri A, the brighter star in the binary, is measured to be $\theta_{\text{A}} = 8.512 \pm 0.022 \text{ mas}$, while that

⁴ Observed parallaxes (and other properties) of some example stars are given in Table B.1 of Appendix B.

⁵ The first interferometric measurement of the angular diameter of Betelgeuse was in 1920, when Michelson and Pease found $\theta_{\text{bet}} = 47 \pm 5 \text{ mas}$ at visible wavelengths.

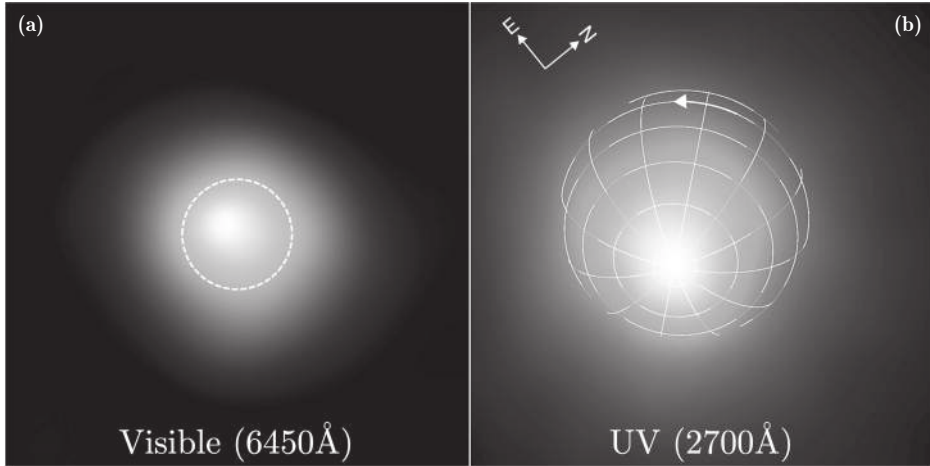


Figure 1.5 (a) Betelgeuse at $\lambda \sim 6450 \text{ \AA}$ (VLT: 2019 Jan). Field of view is $180 \times 180 \text{ mas}$. Dashed circle = size of photosphere. North is up, east is left. [ESO/M. Montargès *et al.* 2021] (b) Betelgeuse at $\lambda \sim 2700 \text{ \AA}$ (*HST*: 1995 Mar). Field of view is $180 \times 180 \text{ mas}$. Overlay indicates the orientation and rotation of Betelgeuse. [Uitenbroek *et al.* 1998]

of α Centauri B is $\theta_B = 6.002 \pm 0.048 \text{ mas}$ and that of Proxima Centauri is $\theta_{\text{prox}} = 1.02 \pm 0.08 \text{ mas}$. Given the distances to these stars, the physical radii of the stars in the binary system are $R_A = 1.22 R_\odot$ and $R_B = 0.86 R_\odot$, while little Proxima Centauri has $R_{\text{prox}} = 0.14 R_\odot$. This means that the radius of Proxima Centauri is only $\sim 40\%$ bigger than that of the planet Jupiter, and is significantly smaller than the radius of puffy “hot Jupiter” exoplanets, swollen by absorbing radiative energy from their nearby parent star.

In addition to having a wide range of sizes, stars have a wide range of rotation speeds. One way to measure the rotation speed v_{rot} of a star is through the rotational broadening of the star’s absorption lines. One problem with using rotational broadening to determine v_{rot} is that the line width tells you only $v_{\text{rot}} \sin i$, where i is the inclination of the star’s rotation axis relative to the line of sight. Since the inclination is not known *a priori*, the line width generally gives only a lower limit on the value of v_{rot} for any particular star. Another problem with using rotational broadening is that the star’s absorption lines also show thermal broadening. For atomic hydrogen, the root mean square thermal speed is

$$v_{\text{th}} = \left(\frac{3kT}{m_{\text{H}}} \right)^{1/2} \approx 12 \text{ km s}^{-1} \left(\frac{T}{5772 \text{ K}} \right)^{1/2}. \quad (1.15)$$

For slowly rotating stars like the Sun, thermal broadening is larger than the rotational broadening. However, for bright stars with high-resolution spectra, thermal broadening can be disentangled from rotational broadening since the